A Theoretical Study of Inner-Shell Photoionization Cross Sections and Angular Distributions

Frank M. Chapman, Jr., and Lawrence L. Lohr, Jr.*

Contribution from the Department of Chemistry, University of Michigan, Ann Arbor, Michigan 48104. Received August 28, 1973

Abstract: Atomic photoionization cross sections and asymmetry parameters are calculated using a simple one-electron model potential consisting of the positive nuclear charge at the origin surrounded by a series of negatively charged spherical shells. The radial Schrödinger equation is solved exactly for unbound states of the potential using Whittaker functions. Parameters for the model potential (shell radii and charges) are fitted using SCF charge densities. Applications are made to inner-shell ionizations of atoms and molecules as observed in ESCA (Mg Kα and Al Kα photon energies), with emphasis on 1s ionizations for boron through neon and 2s and 2p ionizations for aluminum through argon. The periodic variation in cross section for ionization of a given orbital is discussed in terms of the photoelectron kinetic energy. Effects due to core relaxation are considered for the neon atom. The calculations are compared with experimental X-ray absorption coefficients and photoelectron spectral intensities.

Photoelectron spectroscopy using soft X-ray sources has recently become a widely used experimental technique for studying atoms, molecules, and solids.[1] The basic experiment consists of bombarding a sample to be studied with nearly monoenergetic photons and measuring the properties of the ejected photoelectrons. Although most of the emphasis has centered around the energetics of the photoionization process leading to a determination of electron binding energies,[2] with recent advances in the experimental technique it has become feasible to determine the intensity[3] of photoelectron peaks as well as the angular (spatial) distribution[4,5] of the ejected photoelectrons. With these additional parameters the experimentalist can begin to unravel more complex photoelectron spectra.[6] The in-tensity of a photoelectron peak is best described as a cross section, which has the dimensions of area and is a measure of the probability of photoionization occurring from a given orbital at a given photon energy. The angular distribution of the ejected photoelectron is most readily characterized by the asymmetry parameter β.[7]

There have been a number of calculations of photoionization cross sections for molecular valence orbitals. In addition to the work reviewed by Marr,[8] Cohen and Fano have considered the hydrogen molecule ion,[9] Lohr and Robin have treated π-electron systems,[10] while Iwata and Nagakura have recently considered methane, water, and hydrogen sulfide.[11] Angular distributions for photoelectrons ejected from molecular valence orbitals have been considered by Cooper and Zare,[7,12] by Tully, Berry, and Dalton,[13] by

(1) (a) K. Siegbahn, C. Nordling, A. Fahlman, R. Nordberg, K. Hamrin, J. Hedman, G. Johansson, T. Bergmark, S.-E. Karlsson, I. Lindgren, and B. Lindberg, "ESCA; Atomic Molecular and Solid State Structure Studied by Means of Electron Spectroscopy," Almquist and Wiksells, Uppsala, 1967; (b) K. Siegbahn, C. Nordling, G. Johansson, J. Hedman, P. F. Heden, K. Hamrin, U. Gelius, T. Bergmark, L. O. Werme, R. Manne, and Y. Baer, "ESCA Applied to Free Molecules," North-Holland Publishing Co., Amsterdam, 1969.

(2) For example, see D. A. Shirley, *Advan. Chem. Phys.*, 23, 85 (1973).

(3) For example, see G. Wuilleumier and M. O. Krause, "Electron Spectroscopy," Proceedings of the International Conference on Electron Spectroscopy, Asilomar, Pacific Grove, Calif., Sept. 1971, D. A Shirley, Ed., North-Holland Publishing Co., Amsterdam, 1973, pp 259–267 and references contained therein.

(4) T. A. Carlson, G. E. McGuire, A. E. Jonas, K. L. Cheng, C. P. Anderson, C. C. Su, and B. P. Pullen, ref 3, pp 207–231.

(5) T. A. Carlson and A. E. Jonas, *J. Chem. Phys.*, 55, 4913 (1971).

(6) For example, see T. A. Carlson and C. P. Anderson, *Chem. Phys. Lett.*, 10, 561 (1971).

(7) J. Cooper and R. N. Zare, "Lectures in Theoretical Physics," Vol. 11c, S. Geltman, K. Mahanthappa, and W. Brittin, Ed., Gordon and Breach, New York, N. Y., 1969, pp 317–337.

(8) G. V. Marr, "Photoionization Processes in Gases," Academic Press, New York, N. Y., 1967.

(9) H. D. Cohen and U. Fano, *Phys. Rev.*, 150, 30 (1966).

(10) L. L. Lohr and M. B. Robin, *J. Amer. Chem. Soc.*, 92, 7241 (1970).

(11) S. Iwata and S. Nagakura, private communication, to be submitted for publication.

(12) J. Cooper and R. N. Zare, *J. Chem. Phys.*, 48, 942 (1968); 49, 4252 (1968).

(13) J. C. Tully, R. S. Berry, and B. J. Dalton, *Phys. Rev.*, 176, 95 (1968).

Buckingham, Orr, and Sichel,[14] and by Sichel.[15] Our interest here, however, is in calculating cross sections and photoelectron angular distributions for inner-shell (core) photoionization in molecules, with emphasis on photon energies currently used in X-ray photoelectron spectroscopy (ESCA).

The examples we consider are the photoionization of the 1s inner shells of the elements boron through neon and the 2s and 2p inner shells of the elements aluminum through argon by either Mg Kα or Al Kα soft X-rays, with photon energies of 1254 and 1487 eV, respectively. The electron binding energies for these cases range from 90 to 900 eV, so that none of the ionizations considered are close to threshold. Under these circumstances we assume that the photoionization of molecular core electrons can be described as the photoionization of atomic core electrons. Thus we assume for photoelectron kinetic energies ranging from 350 to 1400 eV that we can ignore the effects due to the surrounding molecular environment. Specifically we consider the core levels in a neutral closed shell molecule to be identical with those in neutral atoms with any spin or orbital angular momenta arising from open valence shells of the atoms being ignored. (See the Theoretical Method section.)

There has been a considerable effort devoted to the calculation of atomic photoionization properties,[8,16] with much of this work being for photon energies relevant to natural phenomena. Generally the emphasis has been on either the photoionization of valence electrons in the near threshold region (photon energies less than approximately 50 eV) or photoionizations in the hard X-ray range[17] (photon energies above approximately 10 keV). However, there have been a number of theoretical studies of the soft X-ray photoionization of atoms. Manson and Cooper[18] developed a one-electron model using a Herman–Skillman[19] central potential, which approximated the exchange potential by an effective local potential related to the charge density and calculated cross sections for a number of elements at photon energies ranging from 100 eV to 2 keV. Angular distributions in the soft X-ray range were considered for krypton by Cooper and Manson,[20] leading to the thorough study by Kennedy and Manson[21] of the photoionization cross sections and angular distributions for noble gas atoms at electron kinetic energies from zero to 408 eV (e.g., photon energies up to 734 eV for the 2s shell of argon). In the latter studies the wave functions for the photoelectron were taken as Hartree–Fock functions with complete exchange.

A simpler computational method is that developed by McGuire[22] and based on the exact solution of a piecewise Coulombic potential. This method, which

was used by Heisenberg[23] in an early study of the Rydberg states of helium, is described in detail in the next section as it provides the basis for our own calculations. McGuire reported theoretical cross sections for the ionization of the elements helium to xenon by photons of energies from 6 eV to several kiloelectron volts. However, only the total cross section was listed for each element at a given photon energy, rather than the contributions from each electronic shell, so that the results are not in general useful for comparison with cross sections obtained from photoelectron spectra. In addition no angular distributions were given. In our studies reported here we have used a modification of McGuire's method to calculate photoionization cross sections and angular distribution parameters for inner shells of various elements at soft X-ray photon energies.

Theoretical Method

The general theory of atomic photoionization has been discussed and reviewed by a number of authors[16,24-26] and is presented here only briefly. Since we are restricting our considerations to soft X-ray photon energies ($h\nu < 1500$ eV), we assume that the dipole approximation, equivalent to the neglect of photon momentum, is valid. Krause[27] has presented experimental data for neon 1s ionization showing that the angular distribution differs from that expected for an electric dipole process by not more than 15% with Mg Kα radiation ($h\nu = 1254$ eV) and not more than 20% with Al Kα radiation ($h\nu = 1487$ eV).

Assuming LS coupling for both the initial and final states, an electron initially in the nlth subshell is ionized by an electric dipole process to the continuum with angular momentum $l \pm 1$. The cross section for photoionization of the electron is given in this approximation by

$$\sigma_{nl}(E) = (8\pi^2 \alpha a_0^2 / 3)(I + E)(C_{l-1} R_{l-1}^2 + C_{l+1} R_{l+1}^2) \quad (1)$$

where I (in atomic units) is the ionization energy of the active electron, E (in atomic units) is the energy of the photoelectron ($h\nu = I + E$), α is the fine structure constant, and a_0 is the Bohr radius. The numerical factors $C_{l\pm1}$ arise from integrations over spin and angular coordinates and are tabulated for most cases of interest.[28] The factors $R_{l\pm1}$ are radial matrix elements expressible[29] in either the dipole length or dipole ve-

$$R_{l\pm1} = \int_0^\infty P_{nl}(r) r P_{E,l\pm1}(r) dr \quad (2)$$

locity (gradient divided by transition energy) formula-

$$R_{l\pm1} = \frac{1}{(I+E)} \int_0^\infty P_{nl}(r) \left[\frac{1 \pm (2l + 1)}{2r} P_{E,l\pm1}(r) + \frac{dP_{E,l\pm1}(r)}{dr} \right] dr \quad (3)$$

(14) A. D. Buckingham, B. J. Orr, and J. M. Sichel, *Phil. Trans. Roy. Soc. London, Ser. A*, **268**, 147 (1970).

(15) J. M. Sichel, *Mol. Phys.*, **18**, 95 (1970).

(16) U. Fano and J. W. Cooper, *Rev. Mod. Phys.*, **40**, 441 (1968).

(17) For a recent review, see R. H. Pratt, A. Ron, and H. K. Tseng, *Rev. Mod. Phys.*, **45**, 273 (1973).

(18) S. T. Manson and J. W. Cooper, *Phys. Rev.*, **165**, 126 (1968).

(19) F. Herman and S. Skillman, "Atomic Structure Calculations," Prentice-Hall, Englewood Cliffs, N. J., 1963.

(20) J. W Cooper and S. T. Manson, *Phys. Rev.*, **177**, 157 (1969).

(21) D. J. Kennedy and S. T. Manson, *Phys. Rev. A*, **5**, 227 (1972).

(22) E. J. McGuire, *Phys. Rev.*, **161**, 51 (1967); **175**, 20 (1968). Also see *Phys. Rev. A*, **3**, 267 (1971), for applications to inelastic electron and proton scattering.

(23) W. Heisenberg, *Z. Phys.*, **39**, 499 (1927).

(24) D. R. Bates, *Mon. Notic. Roy. Astron. Soc.*, **106**, 432 (1946).

(25) A. Burgess and M. J. Seaton, *Mon. Notic. Roy. Astron. Soc.*, **120**, 121 (1960).

(26) A. L. Stewart, *Advan. At. Mol. Phys.*, **3**, 1 (1967).

(27) M. O. Krause, *Phys. Rev.*, **177**, 151 (1969).

(28) F. Rohrlich, *Astrophys. J.*, **129**, 441 (1959); **129**, 449 (1959); also see ref 24 and 25.

(29) H. A. Bethe and E. E. Salpeter, "Quantum Mechanics of One- and Two-Electron Atoms," Academic Press, New York, N. Y., 1957, p 249.

tions. The functions $P_{nl}(r)$ and $P_{E,l\pm1}(r)$ are the bound and continuum radial functions $rR_{nl}(r)$ and $rR_{E,l\pm1}(r)$, respectively. The two forms of the matrix element are equal if the bound and continuum wave functions are exact solutions of the same Hamiltonian H (even if the Hamiltonian itself is only approximate in nature) as long as the linear momentum operator is given simply by the product of the electron mass and the quantum mechanical velocity operator $d\mathbf{r}/dt$, the latter being always proportional to the commutator of $\mathbf{r}$ and H. The role of spin–orbit coupling in causing dipole velocity or linear momentum matrix elements to provide a fundamentally invalid description of electric dipole radiative processes has been discussed by Lohr,[30] Englman,[31] and Chiu,[32] while more recently the same role for nonlocal potentials, such as those arising in Hartree–Fock methods, has been discussed by Starace.[33] In our present studies neither spin–orbit nor exchange effects are considered for the continuum wave functions, although our choice of atomic SCF functions to represent the bound state does imply an exchange potential in the effective Hamiltonian for the latter. Our procedure will be seen to combine continuum functions which are exact solutions of a model Hamiltonian without exchange and bound state functions which are inexact solutions of a Hamiltonian with exchange. Thus, as pointed out by Cohen and McEachran,[34] close agreement between the two forms of the matrix element neither is expected nor is a rigorous criterion for wave function exactness. (See the Results and Discussion section.)

The quantity of most direct interest to the experimentalist using photoelectron spectroscopy is the differential cross section $d\sigma_{nl}(E)/d\Omega$, which is a measure of the photoelectron flux observed in a given solid angle $d\Omega$. The differential cross section is related to the total cross section $\sigma_{nl}(E)$ and the asymmetry parameter[7,12] by

$$\frac{d\sigma_{nl}(E)}{d\Omega} = \frac{\sigma_{nl}(E)}{4\pi}\left[1 - \frac{\beta(E)}{4}(3\cos^2\theta - 1)\right] \quad (4)$$

where θ is the angle between the direction of the ejected photoelectron and the direction of the photon beam (assuming unpolarized radiation). Equation 4 essentially describes how the total photoelectron flux is distributed in space, with the exact form of the distribution being characterized by the asymmetry parameter β. This parameter ranges in value from -1 to $+2$, with $\beta = 0$ corresponding to an isotropic (spherical) distribution. For ionization of an electron initally in an s state $\beta = 2$, while for an electron initially in a p state

$$\beta = \frac{2R_2{}^2 - 4R_0R_2\cos(\delta_2 - \delta_0)}{R_0{}^2 + 2R_2{}^2} \quad (5)$$

where R_0 and R_2 are from eq 2 or 3, and δ_0 and δ_2 are phase shifts[21,35] for the s and d states of the photoelectron. General formulas for β corresponding to

ionization of an electron with initial angular momentum l are given elsewhere.[7,12]

The bound state radial functions in eq 2 and 3 are taken as atomic SCF functions, so that the essence of the calculation is the determination of radial functions for the continuum state. A number of methods have been developed for calculating continuum wave functions.[36] We obtain continuum wave functions as solutions to the radial equation

$$\left[-\frac{1}{2}\frac{d^2}{dr^2} - V(r) + \frac{l(l+1)}{2r^2}\right]P_{E,l}(r) = EP_{E,l}(r) \quad (6)$$

where $V(r)$ is the electrostatic potential due to the ionic core

$$V(r) = \frac{+Z}{r} - \frac{1}{r}\int_0^r p(r')dr' - \int_r^\infty \frac{p(r')}{r'}dr' \quad (7)$$

in which $p(r')$ is a radial density related to SCF radial functions $P_{nl}(r) = rR_{nl}(r)$ by

$$p(r') = \sum_{nl}\omega_{nl}P_{nl}(r')^2 \quad (8)$$

Note that we use $V(r)$ to denote the *potential*, so that the potential *energy* is $-V(r)$ in atomic units. The occupation number ω_{nl} for the nlth orbital includes electrons of both spins. However, the summation in (8) does not include the electron being ionized, so that the potential $V(r)$ approaches the correct asymptotic limit of $1/r$. The continuum wave functions are normalized such that[26] as $r \to \infty$, with $k = (2E)^{1/2}$

$$P_{E,l}(r) \longrightarrow (\pi k)^{-1/2}\sin(kr +$$
$$k^{-1}\ln 2kr - l\pi/2 + \delta_l) \quad (9)$$

where δ_l is the phase shift.[21,35] This approach neglects exchange between the continuum electron and the ionic core, as the interaction in eq 7 is purely electrostatic. In addition, the bound state orbitals used in eq 8 are taken as those for the atom before ionization. Thus, the ionization is assumed to be electronically "vertical" (frozen orbital approximation); specifically effects due to relaxation are neglected. (See the Core Relaxation section.)

Solutions to eq 6 are obtained by first determining the potential $V(r)$ in eq 7 and then fitting r times this potential, $rV(r)$, with a series of straight line segments as was done by McGuire.[22] This yields a model potential $V_m(r)$ which is piecewise Coulombic. The procedure is constrained such that the model potential is continuous, the charge at the origin corresponds to actual nuclear charge Z, and the sum of the shell charges equals $1 - Z$; thus, the model potential has the correct form in the limit of large and small r. The fitting is initiated at the origin and propagated outward such that the model and atomic potentials are equal at each of the boundaries; between boundaries the model potential is more positive than the atomic potential. For the results reported here, typically 15 linear segments, corresponding to a nucleus surrounded by 14 spherical shells, are used to fit $rV(r)$ yielding a model potential which differs from $V(r)$ on the average by approximately 0.5%, with a maximum deviation of less than 1.0%. The radius of the outermost shell, beyond

(30) L. L. Lohr, Jr., *J. Chem. Phys.*, **45**, 1362 (1966).
(31) R. Englman, *J. Chem. Phys.*, **45**, 2669 (1966).
(32) Y. N. Chiu, *J. Chem. Phys.*, **48**, 3476 (1968).
(33) A. F. Starace, *Phys. Rev. A*, **3**, 1242 (1971); **8**, 1141 (1973).
(34) M. Cohen and R. P. McEachran, *Chem. Phys. Lett.*, **14**, 201 (1972).
(35) N. F. Mott and H. S. W. Massey, "The Theory of Atomic Collisions," 3rd ed, Oxford University Press, London, 1965, pp 60–65.

(36) For example, see M. J. Seaton, *Phil. Trans. Roy. Soc. London*, *Ser. A*, **245**, 469 (1953), and ref 25.

which the potential is simply $1/r$, is typically located at 3 to 4 bohrs.

Exact continuum solutions to the radial equation for a model potential of the form discussed above are constructed in terms of Whittaker functions. The solution is determined through application of boundary value techniques, requiring continuity of the wave function and its first derivative at each of the potential boundaries. Explicit formulas for the general solution (model potential consisting of any number of shells) have been determined. The Whittaker functions in the variable $(2E)^{1/2}r = kr$ are conveniently evaluated in terms of their power series expansions[37,38] for $kr < 11$ and in terms of asymptotic formulas[39] for $kr > 11$. We have also obtained a general solution for bound states of the piecewise Coulombic potential but have not used it in the studies reported here. Using a similar approach, Gordon[40] has considered exact solutions of the radial equation for a piecewise linear potential for which the solutions are written in terms of Airy functions.

Two computer programs are used in the scheme, the first to calculate the atomic potential and to determine parameters for the model potential and the second to solve the boundary value problem, generate the continuum wave functions, and determine, by numerical integration, the radial matrix elements. During evaluation of the Whittaker functions for $kr < 11$, convergence of the power series expansions is controlled automatically. The Whittaker functions are routinely determined (for all kr) to an accuracy of better than one part in 10^4. The calculation (eq 5) of β requires phase shifts which are readily obtained from the coefficients of the regular and irregular solutions in the outermost region (the shift relative to a pure Coulomb wave) and from standard expressions[35] for the shift of a pure Coulomb wave relative to a free spherical wave.

The bound state wave functions used for the initial state, eq 2 and 3, as well as for determining the atomic potential. eq 7, are Slater basis set SCF functions from Clementi[41] and correspond to the lowest energy term for neutral atoms. The ionization energy I is taken as the negative of the one-electron orbital energy for the electron being ionized (Table I). These values are only approximately Koopmans' theorem ionization energies for those atoms which are open shell. We use these theoretical values rather than experimental ionization energies in order to be consistent with our choice of bound state wave functions.

The angular momentum coupling, which determines the factors $C_{l\pm1}$ in eq 1, is taken as that for closed shell systems. That is, in calculating cross sections for inner shells we neglect the angular momentum of any partially filled outer shells. Thus, our results are in general not applicable to the free atom but to a hypothetical closed shell system, this choice being motivated by our desire to determine cross sections applicable to core ionizations in closed shell molecular systems. All cross sections reported in the next section are for filled

Table I. Ionization Potentials Used in Calculating Photoionization Properties[a]

Atom	Shell	IP, eV
B	1s	209.4
C	1s	308.2
N	1s	425.3
O	1s	562.4
F	1s	717.9
Ne	1s	891.8
Al	2s	133.6
	2p	87.6
Si	2s	167.5
	2p	115.8
P	2s	204.4
	2p	147.0
S	2s	245.0
	2p	181.8
Cl	2s	288.6
	2p	219.6
Ar	2s	335.3
	2p	260.4

[a] Values taken from ab initio orbital energies of ref 41.

inner shells and are *not* to be multiplied by the occupation numbers of 2 and 6 for s and p shells, respectively. Furthermore, since our calculations neglect spin–orbit coupling, the cross sections reported here represent a sum over any spin–orbit split levels for the ionized atom. Although the expression for β, eq 5, specifically assumes LS coupling, it is reasonable to assume that the expression for β is approximately correct for small deviations from LS coupling. We note that experimental efforts at distinguishing different asymmetry parameters for photoelectrons leaving the ion in different spin–orbit states have led to conflicting conclusions.[42,43]

Results and Discussion

As an initial check on our method we compare in Table II cross sections calculated for the neon atom with experimental values. Although we are primarily interested in inner-shell ionizations, we present results for all three shells (1s, 2s, and 2p) at Mg Kα and Al Kα photon energies of 1254 and 1487 eV, respectively. We first note the generally good agreement between results obtained using the dipole length and velocity formulations, with the differences being approximately 1% for the 1s cross sections and 5% for the 2s and 2p cross sections. The differences in the two types of theoretical cross sections reflect differences in the effective one-electron Hamiltonians assumed for bound and continuum states. Indeed when bound states of the piecewise Coulombic potential are computed and used instead of the Slater basis set SCF orbitals, the differences between dipole length and dipole velocity cross sections are always 0.5% or less. This provides a measure of numerical integration errors, as the difference should in principle be zero when both bound and continuum functions are exact solutions of a single Hamiltonian without nonlocal potentials or spin-dependent terms.

The experimental cross sections in Table II are of two types, values obtained from photoelectron spectral intensities[44] and values obtained from X-ray absorption

(37) M. Abramovitz, *Nat. Bur. Stand. (U. S.), Appl. Math. Ser.*, 17, (1952).
(38) A. R. Curtis, *Roy. Soc. Math. Tables*, 11 (1964).
(39) C.-E. Fröberg, *Rev. Mod. Phys.*, 27, 399 (1955).
(40) R. G. Gordon, *J. Chem. Phys.*, 51, 14 (1969).
(41) E. Clementi, *Phys. Rev.*, 127, 1618 (1962), and "Tables of Atomic Functions," an unpublished supplement to *IBM J. Res. Develop.*, 9, 2 (1965).

(42) H. Harrison, *J. Chem. Phys.*, 52, 901 (1970).
(43) H. Harrison, *Bull. Amer. Phys. Soc.*, 15, 1514 (1970).
(44) F. Wuilleumier, *Advan. X-Ray Anal.*, 16, 63 (1973).

Table II. Comparison of Theoretical and Experimental Cross Sections for Neon Atom

Photon energy, eV	Shell	Cross section, Mb[a] Theor[b]	Photoelectron[c]	X-ray[d]	Relative cross section Theor	Photoelectron[c]
1254	1s	0.131 0.132	0.113		67.5 64.4	58.5
1254	2s	0.00635 0.00597	0.00397		3.3 2.9	2.0
1254	2p	0.00194 0.00205	0.00193		1.0 1.0	1.0
1254	Total	0.139 0.140	0.120	0.144		
1487	1s	0.0838 0.0844	0.0709		77.6 74.0	68.2
1487	2s	0.00410 0.00391	0.00265		3.8 3.4	2.5
1487	2p	0.00108 0.00114	0.00104		1.0 1.0	1.0
1487	Total	0.0890 0.0895	0.0746	0.0922		

[a] Cross sections are in megabarns (Mb), 10^{-18} cm^2. [b] The first value corresponds to the dipole length result and the second to the dipole velocity. [c] Values interpolated from photoelectron spectral intensities in ref 44, with estimated uncertainties of 3, 7, and 5% for the 1s, 2s, and 2p cross sections, respectively. [d] Values from X-ray absorption coefficients in ref 45 and containing contributions from 2s and 2p shells.

Table III. Cross Section Ratios and Asymmetry Parameter for Neon 2p

Photon energy, eV	σ_{2s}/σ_{2p}[a]	β Theor[a]	Exptl[b]	$(d\sigma_{2s}/d\Omega)/(d\sigma_{2p}/d\Omega)$ at 90° Theor[a]	Exptl
1254	3.27 2.92	0.74 0.75	0.85	4.14 3.69	2.55,[b] 2.56 (9),[c] 2.9 (2)[d]
1487	3.79 3.43	0.61 0.67	0.76	4.93 4.41	3.22,[b] 3.25 (15),[c] 3.2 (2)[d]

[a] The first value corresponds to the dipole length result and the second to the dipole velocity. [b] Interpolated from data in ref 44. [c] From ref 3, with error values enclosed in parentheses. [d] From ref 1b.

coefficients.[45] We discuss first the photoelectron intensities, obtained using a spectrometer which not only measures the contributions separately from each shell but also separates the intensity for the production of the normal hole state from that for the production of shake-up and shake-off satellites. The experimental values are those reported by Wuilleumier[44] for 89 different photon energies between 50 and 2000 eV. We list in Table II values at 1245 eV based on our linear interpolation of the reported values at 1250 and 1300 eV and values at 1487 eV based on interpolation of the values at 1450 and 1500 eV. We note excellent agreement between the calculated and observed values for the 2p ionization, while the calculated 1s and 2s cross sections are approximately 20 and 50% too high, respectively. All of the theoretical cross sections, but particularly that for the 1s shell, should be modified to take into account relaxation of the core when making these comparisons to photoelectron data. (See the Core Relaxation section.)

The second type of comparison made in Table II is to X-ray absorption cross sections,[45] these including contributions from all shells which can be ionized at a given photon energy. Thus the proper value for comparison with experiment is the sum of cross sections for all three shells. The photon energies here are approximately 1100 eV above threshold for the 2s and 2p shells, whose own contribution to the total atomic cross section amounts to approximately 6%. In contrast, the 1s ionizations are only 350 to 500 eV above threshold and

(45) B. L. Henke and R. L. Elgin, *Advan. X-Ray Anal.*, **13**, 639 (1970); also see the data compliation given by J. H. Hubbell, *At. Data*, **3**, 241 (1971).

provide the major contribution to the total cross section. Agreement between experiment and the total theoretical cross section is good, the latter being only about 4% too small. The 1s cross sections alone are approximately 10% below the experimental total values obtained from X-ray absorption coefficients and thus provide a rough measure of the total cross section at these soft X-ray photon energies.

An additional check of the 2s and 2p cross sections is afforded by comparison of the relative differential cross sections at 90° for these subshells. Using eq 4 this ratio is given by

$$[(d\sigma_{2s}/d\Omega)/(d\sigma_{2p}/d\Omega)]_{90°} = 6(\sigma_{2s}/\sigma_{2p})/(\beta + 4) \quad (10)$$

where β is for the 2p ionization. The calculated ratios, Table III, are approximately 50% larger than the experimental values, a result which implies that either the calculated values of σ_{2s}/σ_{2p} are too large or that the calculated values of β are too small, or both. We have interpolated the recent values of β reported by Wuilleumier[44] for neon 2p ionization, obtaining values of 0.76 at 1487 eV and 0.85 at 1254 eV, with estimated errors of 3% in the measurements. These values are indeed somewhat larger than our values (Table III) of 0.61 or 0.67 at 1487 eV and 0.74 or 0.75 at 1254 eV. The two calculated values at each photon energy correspond to the use of the dipole length and dipole velocity operators, respectively. Using the experimental values of β together with our calculated values of $\sigma(2s)/\sigma(2p)$ reduces by approximately 5% the calculated values of the cross section ratio at 90° from the values given in Table III, but the results are still higher than experiments indicating that the calculated $\sigma(2s)/\sigma(2p)$ ratio is approxi-

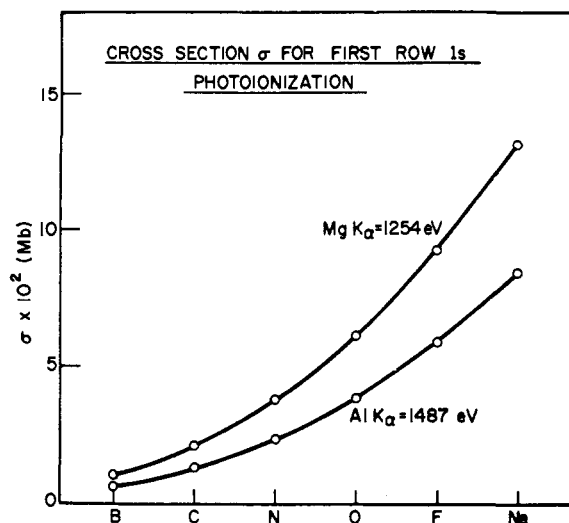*Chapman, Lohr / Inner-Shell Photoionization Cross Sections*

Figure 1. Photoionization cross sections for the 1s shell of first row elements boron to neon. Dipole length and velocity results are essentially identical (Table IV).

Figure 2. Photoionization cross sections for the 2p subshell of second row elements aluminum to argon.

mately 50% too large, as indicated earlier in our comparisons of the calculated individual cross sections to experimental values.

Calculated 1s shell cross sections for the first row elements from boron to neon are summarized in Table IV

Table IV. Comparison of Theoretical and Experimental Cross Sections for First Row 1s[a]

| Atom | hv = 1254 eV | | | hv = 1487 eV | | |
	Theor[b]	Exptl[c]	Diff, %	Theor[b]	Exptl[c]	Diff, %
B	0.0103	0.0114	9.6	0.00631	0.00685	7.9
	0.0103		9.6	0.00621		9.3
C	0.0211	0.0233	9.4	0.0129	0.0143	9.8
	0.0210		9.9	0.0129		9.8
N	0.0376	0.0416	9.6	0.0233	0.0258	9.7
	0.0377		9.4	0.0234		9.3
O	0.0608	0.0672	9.5	0.0382	0.0422	9.5
	0.0614		8.6	0.0384		9.0
F	0.0919	0.1009	8.9	0.0583	0.0644	9.5
	0.0926		8.2	0.0587		8.8
Ne	0.131	0.144	9.0	0.0838	0.0922	9.1
	0.132		8.3	0.0844		8.4

[a] Cross sections are in megabarns, 10^{-18} cm². [b] The first value corresponds to the dipole length result and the second to the dipole velocity. [c] Experimental values are from X-ray absorption coefficients in ref 45 and contain contributions from 2s and 2p shells.

along with experimental values obtained from X-ray absorption coefficients.[45] The experimental cross sections include contributions from the 2s and 2p shells and are for elemental solids (boron and carbon) or gases (nitrogen through neon). As with the neon results in Table II, the calculated 1s shell cross sections are about 10% less than the experimental values but would be raised approximately 6% if contributions from the 2s and 2p shells were added.

In order to understand the variation in 1s shell cross sections from boron to neon (Figure 1), it is useful to have an idea of the various factors affecting the cross sections of an atomic shell. As seen from eq 1 through 3, the cross section depends on the binding energy and shape of the initial, $P_{nl}(r)$, and final, $P_{E,l}(r)$, radial functions of the active electron. Qualitatively, as one
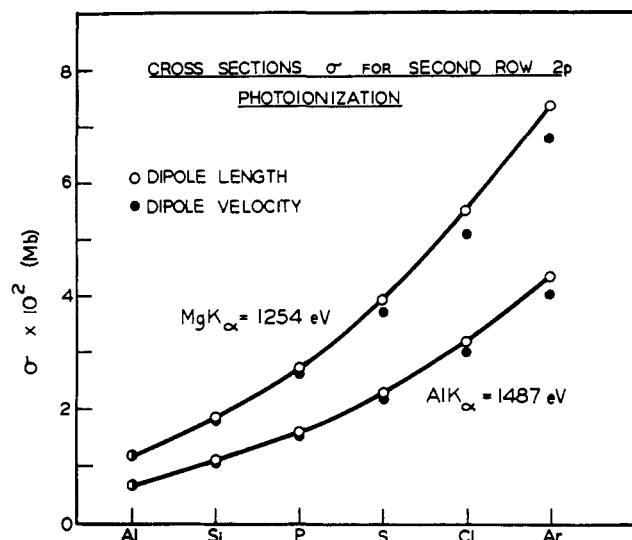
proceeds from boron to neon, the 1s radial functions become more densely concentrated near the nucleus. In an analogous manner the continuum radial functions shift inward toward the nucleus with increasing nuclear charge. In addition, the shape of the continuum function will depend on the energy of the ejected electron and thus on the binding energy of the active electron. Note that the quantity $hv = I + E$ in eq 1 is a constant factor for comparisons at a given photon energy. Calculations at constant photoelectron energy across the first row (1s shell) indicate that a significant part of the variation seen in Figure 1 is due to variation in the photoelectron energy. This seems reasonable since the 1s shell binding energy increases by a factor of 4 going from boron to neon, while the corresponding change in photoelectron energies is a factor of 3.[46] Essentially equivalent considerations are valid for the second row 2s and 2p subshell photoionizations discussed below. Comparing results for Mg Kα and Al Kα, photoionizations with Mg Kα lie approximately 200 eV closer to the 1s shell threshold, so that one observes both a larger magnitude of the cross sections and a larger variation across the row. This is a simple manifestation of the general trend for photoionization cross sections to decrease both in magnitude and in energy variation with increasing photoelectron (or photon) energy.[47]

The variation in photoionization cross sections for the second row 2p subshell is similar to that for the first row 1s shell, with again the photoelectron energy being essentially the controlling factor across the row. However, in this case the ionizations lie approximately 1200 to 1300 eV above the threshold and, as seen in Figure 2, both the magnitude and variation of the cross section is considerably reduced from that of the first row 1s shell. The binding energies and therefore the photoelectron energies (at Mg Kα and Al Kα) for the

(46) We choose to discuss our results in terms of the photoelectron kinetic energy, although one could, of course, choose to emphasize the electron binding energy, the two quantities being related linearly for constant photon energy. Photoelectron energy seems to be the more natural parameter, particularly when one is concerned with the shape of the continuum function and its effect on the cross section.

(47) Some exceptions to this general trend are found to occur within approximately 30 eV of threshold. See, for example, ref 21.
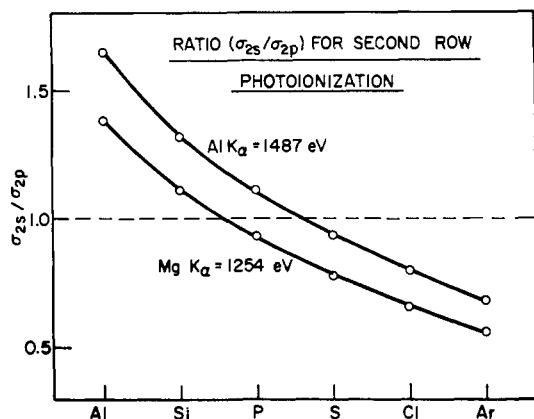
Figure 3. Relative cross sections for the second row 2s and 2p subshells. Dipole length and velocity values of this ratio are essentially identical (Table V).

second row 2s subshell are essentially comparable to those of the second row 2p, and, as seen from Table V,

Table V. Theoretical Cross Sections for Second Row 2s and 2p[a]

Atom	$h\nu = 1254$ eV			$h\nu = 1487$ eV		
	2s[b]	2p[b]	β[b]	2s[b]	2p[b]	β[b]
Al	0.0162	0.0117	1.02	0.0109	0.00660	0.94
	0.0152	0.0116	1.02	0.0103	0.00653	0.94
Si	0.0205	0.0185	1.09	0.0140	0.0106	1.01
	0.0191	0.0177	1.09	0.0131	0.0102	0.01
P	0.0254	0.0273	1.16	0.0175	0.0157	1.08
	0.0235	0.0261	1.16	0.0163	0.0151	1.08
S	0.0304	0.0392	1.22	0.0212	0.0227	1.14
	0.0282	0.0370	1.22	0.0197	0.0216	1.14
Cl	0.0359	0.0549	1.27	0.0253	0.0318	1.20
	0.0333	0.0508	1.27	0.0234	0.0298	1.20
Ar	0.0412	0.0735	1.32	0.0293	0.0431	1.25
	0.0385	0.0678	1.32	0.0273	0.0401	1.25

[a] Cross sections are in megabarns, 10^{-18} cm². [b] The first value corresponds to the dipole length result and the second to the dipole velocity.

the magnitude of the cross section is similar to that of the 2p. It is interesting to note that the relative magnitude of the 2s and 2p cross sections inverts going from Al to Ar, Figure 3. For phosphorus, in particular, there is a crossing of the 2s and 2p cross section curves (vs. photon or photoelectron energy) between Mg Kα and Al Kα. The inversion results, in part, from the greater sensitivity of the 2p cross section to photoelectron energy. A similar inversion of relative cross sections with changing photoelectron energy was observed by Wuilleumier and Krause[3] for the neon 2s/2p ratio.

Included in Table V is the asymmetry parameter β for the second row 2p subshell. The small variation in β across the row as well as the small difference in β for the two photon energies suggests β to be rather insensitive to variation in the photoelectron energy. It should be mentioned, however, that the 2p ionizations are 1200–1300 eV above threshold and that rather dramatic variations in β have been calculated in the energy range close to threshold.[21,48,49] The effect of the angular distribution on the differential cross section, the

(48) S. T. Manson and J. W. Cooper, Phys. Rev. A, 2, 2170 (1970).
(49) S. T. Manson and D. J. Kennedy, Chem. Phys. Lett., 7, 387 (1970).
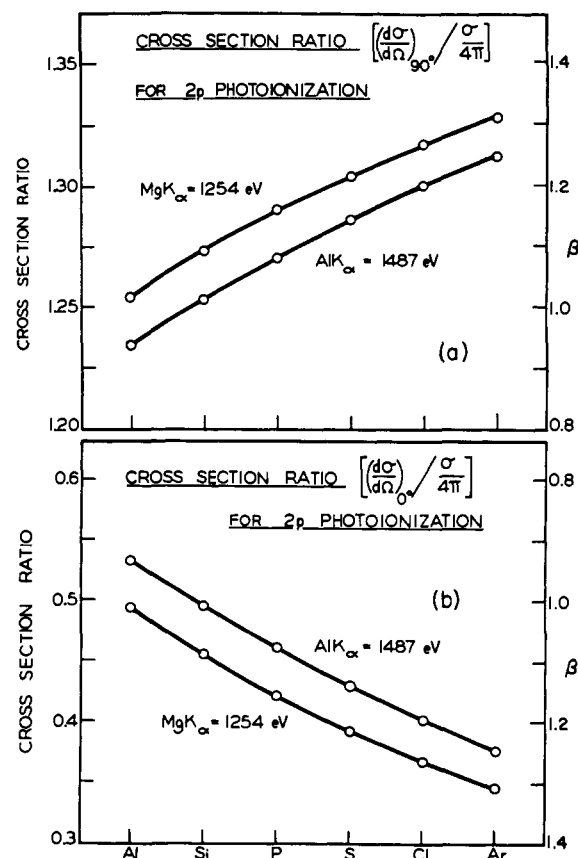

Figure 4. Cross section ratio and asymmetry parameter β for the 2p subshell of second row elements aluminum to argon. Dipole length and velocity results are essentially identical (Table V). In a the photoelectron momentum is perpendicular to the propagation direction of unpolarized light, while in b the photoelectron momentum is parallel to the propagation direction. The left vertical scale in b is one-half that in a, so that the two curves are mirror images.

experimentally accessible quantity in photoelectron spectroscopy, is illustrated in Figure 4 for unpolarized radiation. The cross section ratio is a relative measure of the differential cross section at a given angle $(d\sigma/d\Omega)_\theta$ to the average differential cross section $\sigma/4\pi$. For a spherical distribution $\beta = 0$, and the differential cross section at all angles equals the average differential cross section. As seen from eq 4, for $\theta = 90°$ (Figure 4a, observation perpendicular to the photon beam) the cross section ratio equals $1 + \beta/4$, whereas for $\theta = 0°$ (Figure 4b, observation parallel to the photon beam) the ratio equals $1 - \beta/2$. The left vertical scale in Figure 4b is one-half that in Figure 4a, so that the curves are mirror images of one another and are plots of β (right vertical scales). In connection with the experimental determination of β it should be pointed out that the maximum variation in differential cross section with angle comes at $\theta = 0$. Thus, aside from the fact that for $\beta > 0$ the maximum value of the differential cross comes at $\theta = 90°$, the most sensitive angular region for determining β lies away from $\theta = 90°$.

Since the experimental determination of absolute cross sections necessitates a knowledge of both the photoflux and the density of absorbing species, both formidable experimental problems in the current stage of photoelectron spectroscopy, the most useful applica-

tion of the results presented above is in the relative measurement of cross sections. For example, assuming that two photolines can be measured under comparable experimental conditions, then the ratio of peak intensities for the two lines should equal the corresponding ratio of cross sections. Table VI summarizes all the

Table VI. Relative 1s Shell Cross Sections for Boron to Neon[a]

| Denomi- | Numerator | | | | | |
nator	B	C	N	O	F	Ne
B	1	2.04	3.63	5.88	8.89	12.69
		(2.05)	(3.70)	(6.06)	(9.25)	(13.29)
C		1	1.78	2.88	4.36	6.22
			(1.81)	(2.96)	(4.51)	(6.48)
N			1	1.62	2.45	3.49
				(1.64)	(2.50)	(3.59)
O				1	1.51	2.16
					(1.53)	(2.19)
F					1	1.43
						(1.44)
Ne						1

[a] Values without parentheses are for Mg Kα and values enclosed in parentheses are Al Kα.

possible 1s shell cross section ratios (or their reciprocal) for Mg Kα and Al Kα photon sources. The values without parentheses refer to Mg Kα, with, for example, the ratio of oxygen 1s to carbon 1s being 2.88. The values enclosed in parentheses correspond to Al Kα, where the oxygen 1s to carbon 1s ratio is 2.96. Thomas[50] has reported an experimental oxygen to carbon 1s ratio of 2.21 ± 0.15 using Mg Kα radiation and a gaseous CO sample. He also found the same value for the ratio of the oxygen 1s intensity per atom of oxygen to the carbon 1s intensity per atom of carbon in nitropropane. Our value of 2.88 is definitely higher than his observed value, but not as high as the theoretical ratio of 3.39 which he calculated from Stobbe's formula.[51]

Core Relaxation

The results presented in the preceding section were based on the assumption that the orbitals for the ion are the same as those for the neutral so that the potential energy for the unbound electron in the field of the ion is generated from the charge density of the ion described in terms of these "frozen orbitals." We now explore this approximation, using neon as an example, and relate the results to the question as to whether our cross sections calculated in the frozen orbital approximation are better associated with the contribution of a given shell to an X-ray absorption coefficient or to photoelectron spectral intensities, the latter implying the use of an electron analyzer to select a single final state of the ion.

A consideration of core relaxation introduces three modifications of the procedure for calculating cross sections. Åberg[52] has discussed two of these modifications. First, eq 1 is multiplied by the factor

$$\prod_{nl}\left|\int_0^\infty P_{nl}{}^i(r)P_{nl}{}^f(r)\mathrm{d}r\right|^2 \tag{11}$$

where $P_{nl}{}^i(r)$ and $P_{nl}{}^f(r)$ are orbitals for the initial

(50) T. D. Thomas, *J. Chem. Phys.*, **53**, 1744 (1970).
(51) M. Stobbe, *Ann. Phys. (Leipzig)*, **7**, 661 (1930).
(52) T. Åberg, *Phys. Rev.*, **156**, 35 (1967).

(atom) and final (ion) states, respectively. The product of overlap integrals in (11) is over all orbitals of the ion, meaning that the factor for a given n and l is repeated for each electron in that shell of the ion. The product equals unity in the frozen orbital approximation. Second, the antisymmetry of the total wave functions leads to small correction terms when orbitals for the ion are not orthogonal to orbitals with the same l but different principal quantum n for the neutral atom. However, Åberg has shown[52] that corrections of this type make contributions of approximately 1 part in 10^4, so we have not calculated these corrections. Third, the assumption of a relaxed core implies a change in the attractive potential energy for the photoelectron as compared to that for a frozen core. Thus the continuum wave functions and matrix elements must be recomputed using the potential generated by the charge distribution calculated from orbitals appropriate to the 1s hole state of the ion. Such orbitals are available for neon,[53] and we have used them in obtaining cross sections that include core relaxation effects.

As indicated in Table VII, the cross sections for the

Table VII. Neon 1s Cross Sections Including Core Relaxation

| Photon energy, eV | Cross section, Mb[a,b] | |
	Unrelaxed core	Relaxed core
1254	0.131	0.114
	0.132	0.111
1487	0.0838	0.0729
	0.0844	0.0712

[a] Cross sections are in megabarns (Mb), 10^{-18} cm^2. [b] The first value corresponds to the dipole length result and the second to the dipole velocity.

1s ionization of neon are approximately 15% smaller at each of the photon energies than are the values obtained assuming a frozen core. The square of the one-electron matrix element for the photoactive electron is increased by about 5% when core relaxation is considered (the third effect listed above), meaning that the overlap factor in eq 11 produces more than a 15% reduction. In fact the latter reduction is 21.8%, a value previously obtained by Åberg[52] using the sudden approximation, which may be viewed as a consideration of only the first and second of the three modifications we listed. The reduction in cross section for production of the normal hole state corresponds to the intensity that becomes associated with doubly and multiply excited states of the ion, including both discrete shake-up satellites and the shake-off continuum associated with production of doubly ionized neon with holes in both inner and outer shells. The experimental shake-up intensities for neon reported by Siegbahn, et al.,[1b] using Mg Kα radiation indicate that about 7% of the total intensity of the 1s ionization is associated with discrete shake-up satellites, while the measurements of Krause, et al.,[54] indicate that 18.5 ± 1.0% of the intensity is

(53) Orbitals for neutral neon atom as well as neon ion with a hole in the 1s shell are from P. S. Bagus, *Phys. Rev. A*, **139**, 619 (1965). Ionization potentials for the relaxed and unrelaxed transitions are taken as the total energy difference and Koopmans' theorem [T. Koopmans, *Physica (Utrecht)*, **1**, 194 (1934)] ionization energy, respectively.
(54) M. O. Krause, T. A. Carlson, and R. D. Dismukes, *Phys. Rev.*, **170**, 37 (1968).

associated with discrete and continuous satellites taken together. Krause, *et al.*, also indicate that the probability is about five times greater for double excitation to a continuum state[55,56] of the second electron than to a discrete state so that only about 3% of the 1s ionizations are associated with discrete shake-up satellites, a value less than that reported[1b] by Siegbahn, *et al.*

We do not calculate the probabilities of the two types of double excitations explicitly but simply associate our computed 15% reduction in the normal hole state probability with a rough measure of combined probabilities for double excitations. Thus our results presented in the previous section assuming a frozen core should correspond more closely to the contribution from a given shell of the neutral to intensities measured by experimental techniques such as X-ray absorption, which include transitions to many different final states of the ion having a hole in a specified core orbital, than to photoelectron spectral intensities, since the latter imply the use of an electron energy analyzer to select a single state of the ion. However, relative values of cross sections computed assuming frozen cores, such as the ratios given in Table VI and others that can easily be calculated from our results, should nevertheless serve as a useful guide to photoelectron spectral intensities for inner shells of atoms and molecules.

Summary

We have presented photoionization cross sections at soft X-ray photon energies for the 1s shell of the elements boron through neon and for the 2s and 2p shells

of the elements aluminum through argon. The cross sections were calculated from the exact continuum wave functions of a piecewise Coulombic potential and from reported[41] SCF bound state wave functions. The method for generating the continuum wave functions is very flexible in that various interactions may be added to the potential given in eq 7 before the fitting to a piecewise Coulombic form. Our present use of the method differs from McGuire's[22] in that our fitting is to the purely electrostatic atomic potential generated from SCF charge densities, while his fitting was to Herman–Skillman[19] atomic potentials which include an approximate exchange contribution. Indeed omission of exchange may be a major reason why our 2s cross sections are significantly greater than experimental values at the soft X-ray energies but less than experimental values at lower photon energies. We have found that cross sections for orbitals possessing radial nodes, such as 2s, are more sensitive to changes in the computational method than are cross sections for radially nodeless orbitals, such as 1s and 2p. Calculations including full exchange such as those reported by Kennedy and Manson[21] for noble gases yield results better than ours for the $\sigma(ns)/\sigma(np)$ ratio. In a future publication we shall present photodetachment cross sections for anions calculated by a modification of the present procedure to include both exchange and polarization contributions to the potential.

(55) For measurements of shake-off probabilities, see T. A. Carlson, W. E. Moddeman, and M. O. Krause, *Phys. Rev. A*, 1, 1406 (1970).
(56) For calculations of shake-off probabilities, see T. A. Carlson and C. W. Nestor, Jr., *Phys. Rev. A*, 8, 2887 (1973).

A Theoretical Study of the Tetrahedrane Molecule

Jerome M. Schulman*[1] and Thomas J. Venanzi

Contribution from the Department of Chemistry, Queens College, City University of New York, Flushing, New York 11367. Received January 15, 1974

Abstract: An *ab initio* calculation in the extended Gaussian 4-31G basis set has established that tetrahedrane is a local minimum point on the eight-atom C_4H_4 potential energy surface. The CC and CH bond lengths were found to be 1.48 and 1.05 Å, respectively, after extensive geometry search. A normal coordinate analysis performed in the 4-31G basis furnished predictions of the tetrahedrane vibrational frequencies and the relative ir intensities. Also, a barrier of at least 18 kcal/mol for homolytic cleavage of a single bond has been obtained. The calculated heat of formation, hybridization, photoelectron spectrum, and one-bond nuclear spin–spin coupling constants are given.

Tetrahedrane (tricyclo[1.1.0.0²,⁴]butane), I, is of chemical interest from the viewpoints of: (1) topology, having a carbon framework represented by the simplest connected cubic graph,[2] II; (2) symmetry,[3] having a carbon framework which is the simplest of the five regular polyhedra and one unique skeletal length,

I   II
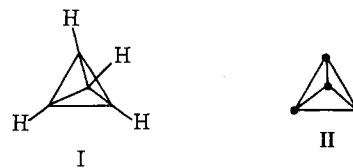
(1) Alfred P. Sloan Research Fellow.
(2) A. T. Balaban, R. O. Davies, F. Harary, A. Hill, and R. Westwick, *J. Aust. Math. Soc.*, 11, 207 (1970).
(3) H. P. Schultz, *J. Org. Chem.*, 30, 1361 (1965).

four being the largest number of points equidistant on the surface of a sphere; (3) quantum theory, as a strained ring system *par excellence*, the fusion of four